Benefit of Measuring Anterior Segment Structures Using an Increased Number of Optical Coherence Tomography Images: The Chinese American Eye Study

Benjamin Y. Xu,[1] Paul Israelsen,[2] Billy X. Pan,[1] Dandan Wang,[1] Xuejuan Jiang,[1] and Rohit Varma[1]

[1]Roski Eye Institute, Keck School of Medicine at the University of Southern California Los Angeles, Los Angeles, California, United States
[2]Keck School of Medicine at the University of Southern California Los Angeles, Los Angeles, California, United States

Correspondence: Benjamin Y. Xu, Department of Ophthalmology, Keck School of Medicine at the University of Southern California, 1450 San Pablo Street, 4th Floor, Los Angeles, CA 90033, USA; benjamin.xu@med.usc.edu.

Submitted: April 18, 2016
Accepted: October 9, 2016

Citation: Xu BY, Israelsen P, Pan BX, Wang D, Jiang X, Varma R. Benefit of measuring anterior segment structures using an increased number of optical coherence tomography images: the Chinese American Eye Study. *Invest Ophthalmol Vis Sci*. 2016;57:6313–6319. DOI:10.1167/iovs.16-19755

Purpose. The purpose of this study was to evaluate the benefit of analyzing an increased number of anterior segment optical coherence tomography (AS-OCT) images on measurement values of various anterior segment parameters.

Methods. Subjects for this cross-sectional study were recruited from the Chinese American Eye Study (CHES), a population-based study in Los Angeles, CA. Thirty-two AS-OCT images were acquired from one eye each of 83 consecutive subjects. Sixteen parameters were analyzed in each image, including angle opening distance (AOD), angle recess area (ARA), trabecular iris space area (TISA), trabecular iris angle (TIA), scleral spur angle (SSAngle), lens vault (LV), pupillary diameter (PD), anterior chamber depth (ACD), anterior chamber width (ACW), iris area (IA), and anterior chamber area (ACA). Data from 1, 2, 4, 8, 16, or 32 OCT images were averaged across subjects to calculate the range and mean of measurement values for each parameter.

Results. Anatomical variations were poorly captured with fewer OCT images for AOD, ARA, TISA, SSAngle, IA, and LV. For these parameters, the range and mean of measurement values obtained from one OCT image deviated from 32-image values by up to 43.9% and 13.3% of the 32-image mean, respectively. These deviations decreased when additional OCT images were analyzed. Deviations from 32-image range and mean values were less pronounced regardless of image number for PD, ACD, ACW, and ACA, measuring up to 3.5% and 5.0%, respectively.

Conclusions. A multi-image approach should be the standard in OCT-based studies of AOD, ARA, TISA, TIA, SSAngle, IA, and LV.

Keywords: anterior segment anatomy, anterior segment OCT, imaging methods

Anterior segment optical coherence tomography (AS-OCT) is a recently invented imaging method that acquires cross-sectional images of anterior segment structures by measuring their optical reflections.[1] The technology has rapidly increased in popularity among clinicians and researchers, especially as a means of studying the anatomy and biomechanics of the anterior chamber. AS-OCT imaging has provided insight into a wide variety of topics including anatomical changes after pupillary dilation and peripheral iridotomy, postsurgical changes after cataract surgery and trabeculectomy, and the relationship between intraocular pressure and the configuration of the anterior chamber angle.[2–12]

Although the topics investigated using AS-OCT have been diverse, limited work has been done to elucidate the anatomical variations inherent in various anterior segment parameters or to quantify the number of OCT images needed to accurately measure each parameter. Most AS-OCT studies represent the anterior segment by using a single cross-sectional OCT image acquired along the temporal-nasal meridian. There are several reasons why this approach is more prevalent than a multi-image approach. Early time-domain and Fourier-domain AS-OCT had to sacrifice acquisition speed for spatial resolution due to technological limitations.[13] Additionally, early AS-OCT studieguyis reported poor reliability and reproducibility when imaging the vertical portions of the angle, although more recent work supports the contrary.[14–19]

Recent advances in OCT technology have removed many of the barriers to acquiring a more robust image representation of the anterior segment. Modern swept-source Fourier-domain AS-OCT devices, such as the CASIA SS-1000 (Tomey Corp., Nagoya, Japan), can acquire up to 128 cross-sectional OCT images in a matter of seconds. Although the available number of OCT images has dramatically increased, the impact of analyzing additional images on measurement values remains unclear for most anterior segment parameters. Ideally, increasing the number of images makes measurements more sensitive to anatomical variations. Realistically, this benefit is limited by several factors. There is a finite amount of anatomical variation within the anterior chamber angle, which means that data beyond a certain point will be redundant. Also, reliance of current analysis methods on manually identifying the scleral spur in each image means that additional analysis time and measurement error offsets the benefit of analyzing more OCT images.

This study examines the relationship between the number of anterior segment OCT images analyzed and measurement

Investigative Ophthalmology & Visual Science

values obtained. We examine this relationship for an extensive list of anterior segment parameters that comprises the majority of parameters that are currently studied. We hypothesize that analyzing fewer images may misrepresent anatomical variations and lead to inaccurate measurements for some if not all parameters.

Methods

Eighty-three consecutive subjects were recruited from the Chinese American Eye Study (CHES), which was a population-based, cross-sectional study that included 4570 Chinese participants 50 years of age and older residing in the city of Monterey Park, CA, USA.[20] As participants of CHES, each subject received a complete eye examination by an ophthalmologist, which included, in order, Goldmann applanation tonometry, gonioscopy, and AS-OCT imaging.[20] Subjects with a history of eye procedures, including laser peripheral iridotomy and cataract surgery, were excluded. Intraocular pressure (IOP) was not an exclusion criteria. Ethics committee approval was previously obtained from the University of Southern California Medical Center Institutional Review Board. All study procedures adhered to the tenets of the Declaration of Helsinki.

Two-dimensional OCT images were acquired using the CASIA SS-1000 swept-source Fourier-domain OCT device (Tomey Corp.). Imaging of both eyes was performed in all subjects under standardized dark-room conditions prior to pupillary dilation. One eye from each subject was randomly selected for analysis using MATLAB (Mathworks, Natick, MA, USA). Raw image data were imported into the SS OCT viewer software (version 3.0; Tomey Corp.), which automatically segmented the anterior segment structures and produced measurements of the anterior segment parameters once the scleral spurs were marked. The software was capable of saving segmentation and scleral spur data for up to 32 of 128 images acquired, which defined the upper limit of number of images analyzed. Data were exported in an Excel (Microsoft, Redmond, WA, USA) format file. The first image analyzed was oriented along the horizontal (temporal-nasal) meridian. Additional OCT images were evenly spaced apart from the horizontal meridian: 90° for 2 images, 45° for 4 images, 22.5° for 8 images, 11.3° for 16 images, and 5.1° for 32 images.

Two observers (PI and BXP), masked to the identities and examination results of the subjects, confirmed the structure segmentation and marked the scleral spurs in each image. The scleral spur was defined as the inward protrusion of the sclera where a change in curvature of the corneoscleral junction was observed.[21]

Data from 16 anterior segment parameters were analyzed using MATLAB. Ten parameters described the angle, as follows: angle opening distance (AOD), angle recess area (ARA), trabecular iris space area (TISA), trabecular iris angle (TIA), and scleral spur angle (SSAngle) measured at 500 μm and 750 μm from the scleral spur. Six parameters described different properties of the anterior chamber: iris area (IA), anterior chamber depth (ACD), lens vault (LV), anterior chamber width (ACW), pupillary diameter (PD), and anterior chamber area (ACA).[8,22] Interobserver and intraobserver reproducibility of measurement values were calculated in the form of intraclass correlation coefficients (ICCs) for each parameter, using data derived from eight common eyes.

Measurement values for all individual eyes were pooled and averaged for each of the 32 cross-sectional images of the anterior chamber. Each OCT image produced a single value for ACD, LV, ACW, PD, and ACA and 2 values for AOD, ARA, TISA, TIA, SSAngle, and IA. These data were normalized for all anterior segment parameters according to the mean measurement value derived from 32 images. These data were then plotted moving from nasal to superior to temporal to inferior to nasal again. Plots of AOD 750 μm (AOD750) and ACW developed by using data points derived from fewer OCT images (1, 2, 4, 8, and 16 images) were produced for comparison with plots derived from 32 images.

The main outcome measurements of the study were the ranges and means of measurement values obtained from an increasing number of OCT images. The range of measurement values was calculated by subtracting the minimum measurement value from the maximum measurement value obtained from 1, 2, 4, 8, 16, or 32 OCT images. Each range was then recalculated as a percentage of the 32-image mean. The deviation of the range was calculated by subtracting the range obtained from 1, 2, 4, 8, or 16 images from the 32-image range. The mean measurement values were calculated by averaging all measurement values along the angle obtained from 1, 2, 4, 8, 16, or 32 OCT images. Each mean was then recalculated as a percentage of the 32-image mean. The deviation of the mean was calculated by subtracting the mean measurement value obtained from 1, 2, 4, 8, or 16 images from the 32-image mean.

Results

Optical coherence tomography images from 83 individual eyes, 42 (51%) right and 41 (49%) left, were analyzed for this study. Observer 1 analyzed 43 eyes (52%), and observer 2 analyzed 40 eyes (48%). The subjects ranged from 50 to 87 years of age (mean = 61 years of age). Forty subjects (48%) were male, and 43 (52%) were female. Intraocular pressure ranged from 6 to 31 mm Hg (mean IOP = 14.3 ± 3.6 mm Hg). The average gonioscopy grade was 2.9 ± 0.6. Six subjects (7.2%) had occludable angles (defined as pigmented trabecular meshwork that could not be visualized for at least half of the angle circumference). Average axial length was 24.3 ± 1.4 mm, and central cornea thickness was 560 ± 38 μm. In total, 2656 cross-sectional OCT images (83 eyes × 32 images) were analyzed. Of these images, 140 (5.3%) were excluded from the final analysis because at least one scleral spur could not be identified.

Interobserver ICC values reflected various degrees of correlation among the parameters.[23] Two parameters showed fair correlation (ICC = 0.40 to 0.59): ARA 500 μm (ARA500; ICC = 0.52), ARA750 (ICC = 0.55). Four parameters showed good correlation: AOD 500 μm (500AOD) (ICC = 0.69), TISA500 (ICC = 0.64), TISA750 (ICC = 0.69), ACW (ICC = 0.62). Ten parameters showed excellent correlation (ICC = 0.75 to 1.00): AOD750 (ICC = 0.78), TIA500 (ICC = 0.75), TIA750 (ICC = 0.82), SSAngle500 (ICC = 0.75), SSAngle750 (ICC = 0.82), LV (ICC = 0.92), PD (ICC = 0.99), ACD (ICC = 0.84), IA (ICC = 0.85), and ACA (ICC = 0.99).

Intraobserver ICC values reflected excellent correlation for all parameters. Intraclass correlation coefficient values ranged between 0.95 (TIA500, SSAngle500) and 0.99 for observer 1 and between 0.91 (TIA500) and 0.99 for observer 2.

Variations of Measurement Values Along the Angle

Thirty-two image plots of the entire angle averaged across all subjects revealed substantial variation of measurement values along the angle for some anterior segment parameters (Fig. 1). This variation was most noticeable among the plots of the angle parameters (AOD, ARA, TISA, TIA, and SSAngles at 500 μm and 750 μm). On average, angles were most narrow superiorly and inferiorly and most open temporally and nasally,

Investigative Ophthalmology & Visual Science

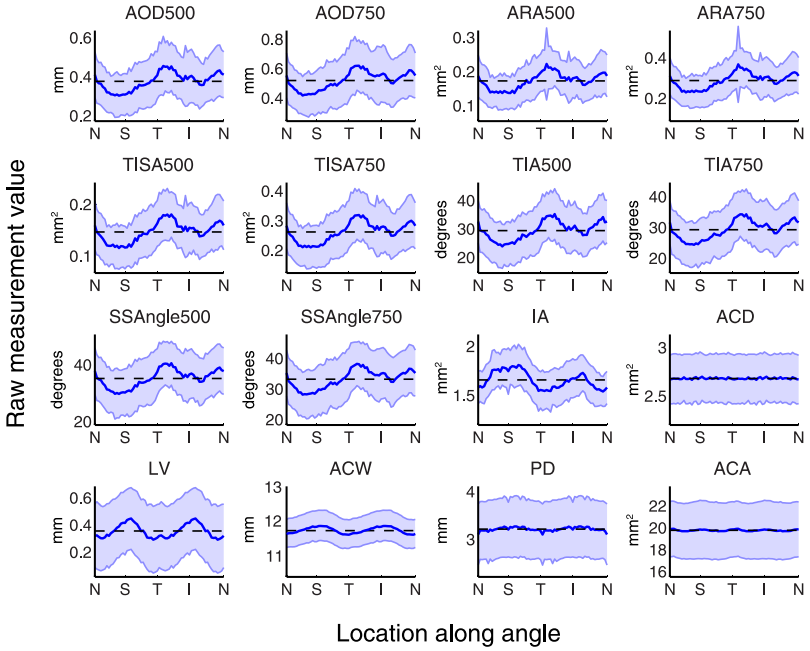

Figure 1. Anatomical variations of 16 anterior segment parameters plotted using measurements obtained from 32 OCT images. Data represent 32-image AS-OCT from 86 subjects pooled and averaged to calculate mean measurement values (*blue lines*) and standard deviation values (*blue bars*) at each of 64 evenly spaced locations along the angle for 16 anterior segment parameters. Each plot represents a different parameter and is centered on the mean of all measurement values that make up the curve (*dashed lines*). Parameters that demonstrated relatively large amounts of anatomical variability along the angle include AOD, ARA, TISA, TIA, SSAngle, IA, and LV. ACD, ACW, PD, and ACA demonstrated relatively small amounts of anatomical variability.

difference ranging from 30.4% (SSAngle750) to 50.0% (ARA500) of the 32-image mean.

Among the remaining six anterior chamber parameters, 32-image plots of IA and LV measurement values demonstrated noticeable anatomical variations. Lens vault was greatest along the vertical meridian and least along the horizontal meridian, with a range of 43.9%. The iris was thickest superiorly and inferiorly and thinnest temporally and nasally, with a range of 16.3%. Measurement values for ACW, ACD, PD, and ACA did not vary dramatically along the angle, ranging from 1.1% (ACA) to 4.9% (PD).

AOD750 and ACW Measured With an Increasing Number of OCT Images

Representative plots of AOD750 were generated to visualize the impact of an increasing number of OCT images on the range and mean of measurement values for a parameter demonstrating a large degree of anatomical variation. Plots more closely approximated the 32-image plot as the number of OCT images and data points increased (Fig. 2, top). One OCT image poorly approximated the anatomical variations of the angle, which was reflected in the deviation of the range and mean of measurement values from 32-image values (29.8% and 11.3%, respectively). These deviations diminished as the number of OCT images increased. When data from eight or more images were plotted, the two curves and their range of values became nearly indistinguishable (deviations of less than 0.8%).

Representative plots of ACW were generated to visualize the impact of an increasing number of OCT images on the range and mean of measurement values for a parameter demonstrating a small degree of anatomical variation. Plots of ACW closely approximated the 32-image plot of ACW, even when the number of OCT images and data points representing the angle were low (Fig. 2, bottom). The ranges and means of measurement values obtained from one OCT image deviated by 3.6% and 1.6%, respectively, from 32-image values. These deviations decreased to 0.3% or less with two or more images.

Deviation of Measurement Value Ranges From 32-Image Range

Plots representing the deviations of measurement value ranges from 32-image ranges for an increasing number of OCT images looked similar for all 10 angle parameters, which included AOD, ARA, TISA, TIA, and SSAngle at both 500 and 750 μm (Fig. 3). Deviations of single OCT ranges from 32-image ranges varied based on parameter, from 25.0% (SSAngle 750 μm) to 40.6% (ARA500). When the number of OCT images was increased to two, all deviations decreased and varied from 6.5% (AOD500 and TISA500) to 11.8% (ARA750). Deviations continued to decrease with four images and varied between 3.5% (AOD750 and SSAngle750) and 11.5% (ARA500). All deviations were 5.0% or less with eight or more images.

Aside from IA and LV, deviations of measurement value ranges for anterior chamber parameters (ACW, PD, ACD, and ACA) were less affected by an increase in the number of OCT images than for angle parameters (Fig. 3). Lens vault and IA were the only parameters that deviated by more than 5.3% from the 32-image range with one OCT image (43.9% for LV; 14.6% for IA). All anterior chamber parameters, except for LV, were stable within 2.1% of the 32-image range with two or more OCT images. Lens vault deviated by 11.3% with 2 and 4 images, 5.0% with 8 images, and 1.7% with 16 images.

Deviation data plotted separately for the two observers approximated the overall data for all parameters. The median and maximum interobserver differences in deviations among all parameters were, respectively, 4.7% and 18.3% with 1 image, 1.9% and 7.1% with 2 images, 0.7% and 7.3% with 4 images, 1.6% and 4.6% with 8 images, and 0.7% and 4.0% with 16 images.

Investigative Ophthalmology & Visual Science

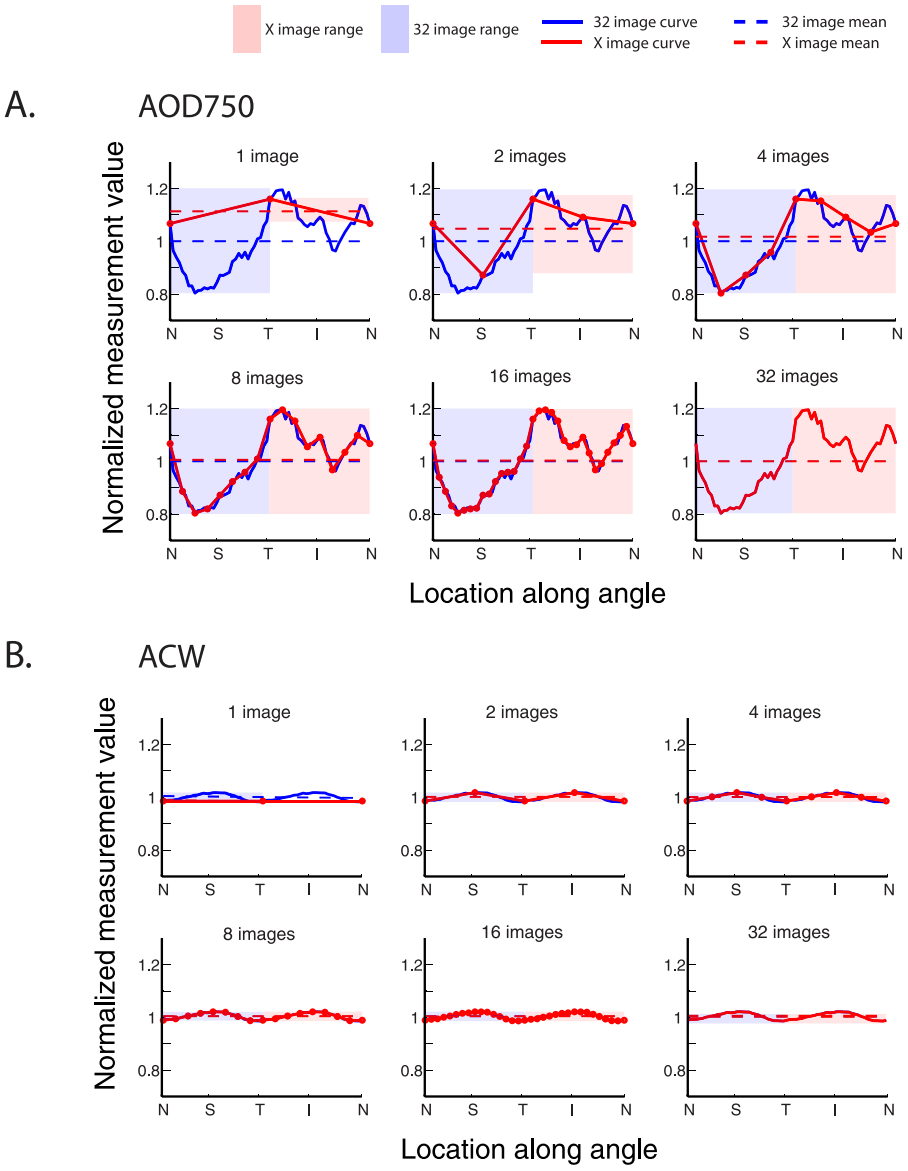

Figure 2. Mean and range of measurement values plotted using an increasing number of OCT images for a high-variability (AOD750) and low-variability (ACW) parameter. (**A**) Each plot compares measurement values derived from 32 images (*solid blue line*) with values derived from fewer images (1, 2, 4, 8, 16 images) for the AOD750 parameter. The mean measurement value, equal to the average of all measurement values obtained from 32 (*dotted blue lines*) or fewer images (*dotted red lines*) and the range of measurement values, equal to the peak-to-trough values obtained from 32 (*blue boxes*) or fewer images (*red boxes*), are also plotted. The differences between measurement value means and ranges are pronounced when just one OCT image is analyzed but decrease as the number of OCT images analyzed increases. (**B**) A similar comparison is made for the ACW parameter, plotted according to the same conventions. The differences between measurement value means and ranges are small, even when just one OCT image is analyzed.

Deviation of Measurement Value Means From 32-Image Means

Plots representing deviations of measurement value means from the 32-image means for an increasing number of OCT images appeared to be similar for all 10 angle parameters (Fig. 4). Deviations of single OCT means from 32-image means ranged from 8.8% (SSAngle 750 μm) to 13.3% (AOD500). When the number of OCT images was increased to two, all deviations of the means decreased, ranging from 2.8% (ARA500 and TISA500) to 5.6% (AOD750). All angle parameters achieved deviations of 1.7% or less with 4 images, 0.6% or less with 8 images, and 0.3% or less with 16 images.

Aside from LV, deviations of measurement value means for anterior chamber parameters were less affected by an increase in the number of OCT images than for angle parameters (Fig. 3). Lens vault and IA were the only parameters that deviated by more than 3.5% of the 32-image mean with one OCT image (10.1% for LV, 5.3% for IA). All anterior chamber parameters except LV were stable within 1.1 % of the 32-image mean with 2 or more OCT images. LV deviated by 6.2% with 2 images, 2.0% with 4 images, and by 0.6% or less with 8 or more images.

Deviation data plotted separately for the two observers approximated the overall data for all parameters. The median and maximum interobserver differences in deviations were, respectively, 3.3% and 6.2% with 1 image, 1.3% and 2.6% with 2 images, 0.3% and 2.2% with 4 images, 0.1% and 1.0% with 8 images, and 0.1% and 0.5% with 16 images.

Investigative Ophthalmology & Visual Science

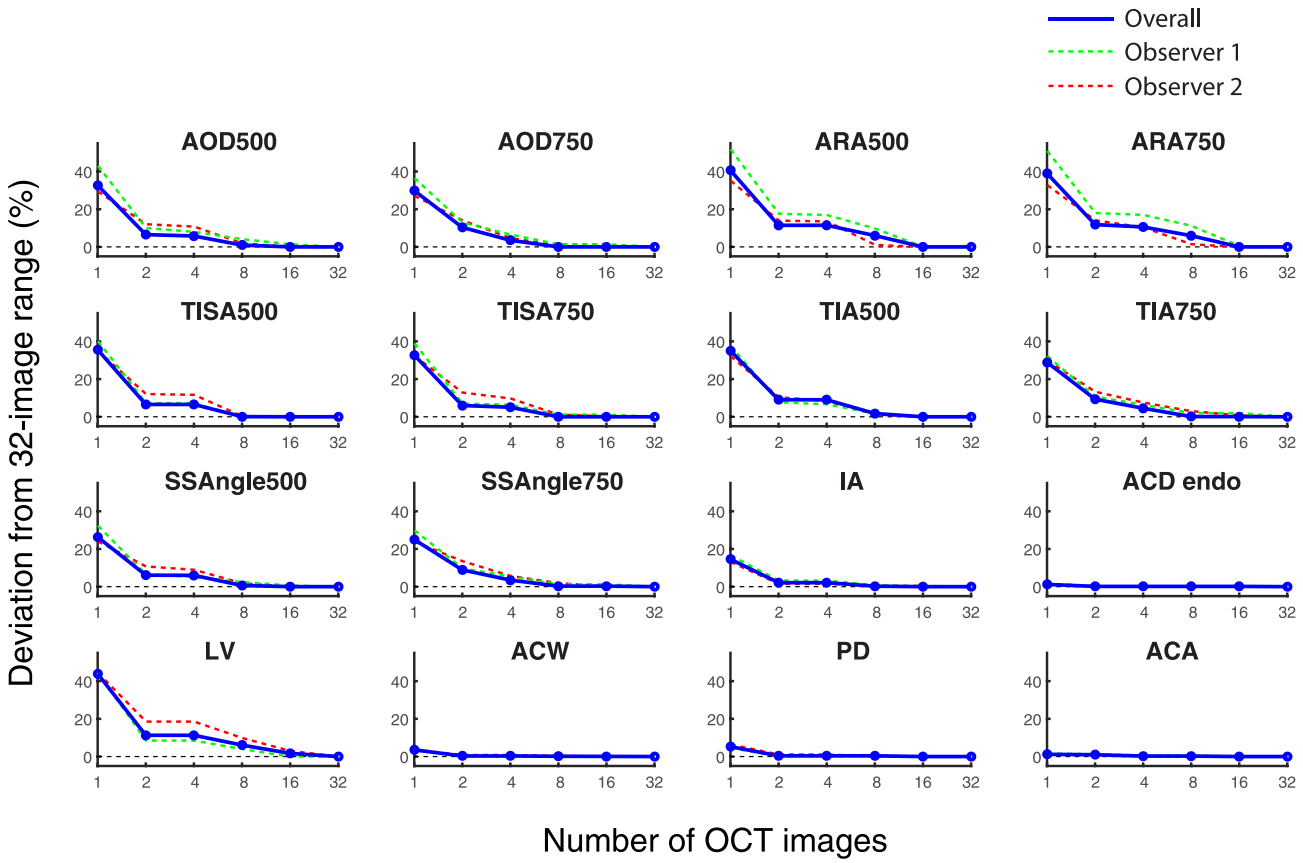

Figure 3. Deviations of measurement value range for an increasing number of images. The deviations of range values obtained from an increasing number of images compared to 32-image values are plotted for 16 anterior segment parameters. Overall deviations (*red lines*) and individual observer deviations (*green line* is observer 1; *red line* is observer 2) are shown. As the number of OCT images increased for AOD, ARA, TISA, TIA, SSAngle, IA, and LV, deviations of the mean and range values decreased. Deviation values were minimal for ACD, ACW, PD, and ACA, even when one OCT image was analyzed.

Discussion

We examined the relationship between the number of OCT images analyzed and the measurement values obtained for an extensive list of anterior segment parameters. First, we identified substantial anatomical variations along the length of the angle that are evident when measurement values are plotted using data obtained from 32 OCT images. We then showed that these anatomical variations are misrepresented for the majority of parameters when structures are measured with one OCT image. Finally, we demonstrated that a multi-image approach to measuring anterior segment structures provides a benefit in terms of approximating anatomical variations even when the number of images analyzed is fewer than 32.

The results of this study are crucial in light of the fact that there is no standardized method to guide OCT-based studies of angle anatomy: many AS-OCT studies of the anterior chamber angle are conducted using one OCT image based on convention. Our results strongly suggest that analyzing 1 or even 2 OCT images is insufficient to characterize the anatomical variations inherent in most anterior segment parameters describing a population of Chinese American eyes. Measuring the angle with fewer OCT images leads to errors in the range and mean of measurement values that could give a misleading impression of whether an angle is open, narrow, or closed. This has broad implications, especially for those studying the relationship between narrow angles and angle closure glaucoma.

While it is intuitive that analyzing an increased number of images could affect measurement values of some parameters, which parameters warrant a multi-slice approach is not well studied. One previous study examined 23 multiethnic eyes with narrow angles and concluded that at least 16 OCT images were necessary to accurately represent a volumetric parameter, the trabecular-iris circumferential volume.[24] As our results demonstrate, such a large number of images is not necessary to study other parameters. Also, we believe that our analysis of more commonly used parameters has broader utility since it is not known which parameters best correlate with the development of conditions such as primary angle closure glaucoma.

The results of our study confer a significant time-saving benefit given the current, semiautomated approach to analyzing AS-OCT images. Manually marking the scleral spur in each OCT image is a time-consuming process that previously provided an unclear benefit. Our results demonstrate that a modest increase in the number of cross-sectional images analyzed provides a noticeable benefit in terms of measurement accuracy. We recommend analyzing at least 4 OCT images when studying the mean of measurement values and 8 OCT images when studying the range of measurement values for the high variability parameters. These numbers of OCT images provide a balance between capturing anatomical variations and increasing data analysis time.

Our study is the first to plot the anatomical variations of conventional angle parameters using 32 OCT images, with four images being the previous high.[25] This novel analysis approach

Investigative Ophthalmology & Visual Science

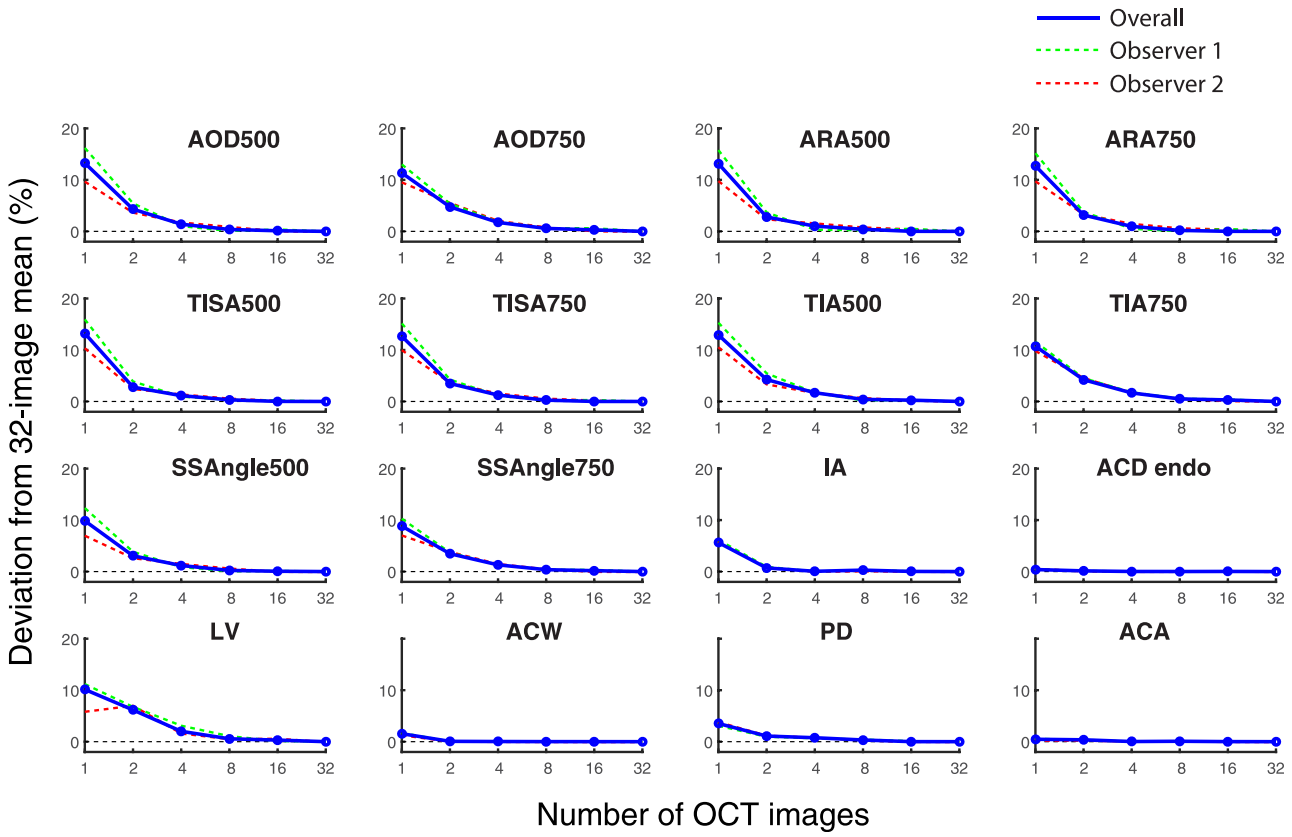

Figure 4. Deviations of measurement value means for an increasing number of images. The deviations of mean values obtained from an increasing number of images compared to 32-image values are plotted for 16 anterior segment parameters. Both the overall deviations (*red lines*) and the individual observer deviations (*green line* is observer 1; *red line* is observer 2) are shown. As the number of OCT images increased for AOD, ARA, TISA, TIA, SSAngle, IA, and LV, deviations of the mean values decreased. Deviation values were minimal for ACD, ACW, PD, and ACA, even when one OCT image was analyzed.

permits resolution of fine anatomical variations in the angle and reveals interesting points about angle anatomy that have not previously been described. First, the value of LV, defined as the distance from the anterior surface of the lens to a straight line drawn through both scleral spurs, varies throughout the length of the angle. This implies that the position of the scleral spur is not constant along the angle but rather varies along the anterior-posterior axis. Based on LV measurements, the scleral spur is more recessed along the superior-inferior meridian than the temporal-nasal meridian, which may explain the previous observation that the trabecular meshwork is wider in the superior and inferior quadrants compared to the temporal and nasal quadrants.[26] Second, the most open (inferotemporal) and narrowest (superonasal) portions of the angle are off-centered from the cardinal meridians and occur at locations that are not typically imaged. Identifying and studying these specific portions of the angle could play a crucial role in accurately assessing a patient's risk for conditions such as angle closure glaucoma. These types of insights into the fundamental basis of anterior segment anatomy cannot be made using traditional investigational methods such as gonioscopy, ultrasound biomicroscopy, or EyeCam (Clarity Medical Systems, Pleasanton, CA, USA), and support a greater role for multi-image AS-OCT.[25,27,28]

We acknowledge a number of limitations to our study. First, interobserver and intraobserver variabilities in marking the scleral spur are inherent limitations in the analysis of AS-OCT images. However, 14 of 16 interobserver ICC values reflected good to excellent correlation, and all 16 intraobserver ICC values for our two observers reflected excellent correlation.[23] These values were consistent with previously reported values.[17] Also, despite these sources of measurement variability, the benefit of analyzing additional images was consistent across observers even for parameters that had relatively low ICC values. Second, our study population consisted of only Chinese American subjects. The anatomical variations in our study may not be generalizable to different races, and therefore, the impact of analyzing an increasing number of OCT images also may not be generalizable. Third, we did not select or separate subjects based on gonioscopic grade. It is conceivable that the number of OCT images necessary to accurately represent a population of narrow angles could differ from the number derived from this study population. Finally, due to technical limitations, we were unable to save, transfer, and analyze data from more than 32 OCT images. Analyzing 64 or 128 images could yield significantly different measurement values than analyzing 32 images, but we believe this to be unlikely given the stability of measurement value means and ranges achieved with only four and eight images, respectively.

This study represents the first step toward establishing a standardized method for OCT-based studies of anterior segment anatomy. Our results clearly demonstrate the benefit and importance of a multi-image approach to OCT-based studies of the anterior segment. It is important to note that, although we argue for a minimum number of images to be analyzed in future studies, we do not argue for a maximum number of images. In fact, we believe that as image processing algorithms become available that automate the identification of anterior segment structures, including the scleral spur, multi-image AS-OCT studies will become standard practice.[29] However, given the limitations imposed by the current semi-

automated experimental approach, we believe there is a benefit to knowing the number of images that should be analyzed to achieve a more accurate representation of anatomical variations among anterior segment structures.

Acknowledgments

Supported by National Institutes of Health/National Eye Institute Grant EY-017337 and a Research to Prevent Blindness, Inc., unrestricted grant. Rohit Varma is a Research to Prevent Blindness Sybil B. Harrington Scholar.

Disclosure: **B.Y. Xu**, None; **P. Israelsen**, None; **B.X. Pan**, None; **D. Wang**, None; **X. Jiang**, None; **R. Varma**, None

References

1. Izatt JA, Hee MR, Swanson EA, et al. Micrometer-scale resolution imaging of the anterior eye in vivo with optical coherence tomography. *Arch Ophthalmol*. 1994;112:1584–1589.
2. Seager FE, Jefferys JL, Quigley HA. Comparison of dynamic changes in anterior ocular structures examined with anterior segment optical coherence tomography in a cohort of various origins. *Invest Ophthalmol Vis Sci*. 2014;55:1672–1683.
3. Dastiridou AI, Pan X, Zhang Z, et al. Comparison of physiologic versus pharmacologic mydriasis on anterior chamber angle measurements using spectral domain optical coherence tomography. *J Ophthalmol*. 2015;2015:845643.
4. Mak H, Xu G, Leung CK-S. Imaging the iris with swept-source optical coherence tomography: relationship between iris volume and primary angle closure. *Ophthalmology*. 2013;120:2517–2524.
5. Han S, Sung KR, Lee KS, Hong JW. Outcomes of laser peripheral iridotomy in angle closure subgroups according to anterior segment optical coherence tomography parameters. *Invest Ophthalmol Vis Sci*. 2014;55:6795–6801.
6. Jiang Y, Chang DS, Zhu H, et al. Longitudinal changes of angle configuration in primary angle-closure suspects: the Zhongshan Angle-Closure Prevention Trial. *Ophthalmology*. 2014;121:1699–1705.
7. Kronberg BP, Rhee DJ. Anterior segment imaging and the intraocular pressure lowering effect of cataract surgery for open and narrow angle glaucoma. *Semin Ophthalmol*. 2012;27:149–154.
8. Mansouri M, Ramezani F, Moghimi S, et al. Anterior segment optical coherence tomography parameters in phacomorphic angle closure and mature cataracts. *Invest Ophthalmol Vis Sci*. 2014;55:7403–7409.
9. Shao T, Hong J, Xu J, Le Q, Wang J, Qian S. Anterior chamber angle assessment by anterior-segment optical coherence tomography after phacoemulsification with or without goniosynechialysis in patients with primary angle closure glaucoma. *J Glaucoma*. 2015;24:647–655.
10. Hamanaka T, Omata T, Sekimoto S, Sugiyama T, Fujikoshi Y. Bleb analysis by using anterior segment optical coherence tomography in two different methods of trabeculectomy. *Invest Ophthalmol Vis Sci*. 2013;54:6536–6541.
11. Nakashima K-I, Inoue T, Fukushima A, Hirakawa S, Kojima S, Tanihara H. Evaluation of filtering blebs exhibiting transconjunctival oozing using anterior segment optical coherence tomography. *Graefes Arch Clin Exp Ophthalmol*. 2015;253:439–445.
12. Chong RS, Sakata LM, Narayanaswamy AK, et al. Relationship between intraocular pressure and angle configuration: an anterior segment OCT study. *Invest Ophthalmol Vis Sci*. 2013;54:1650–1655.
13. Asrani S, Sarunic M, Santiago C, Izatt J. Detailed visualization of the anterior segment using fourier-domain optical coherence tomography. *Arch Ophthalmol*. 2008;126:765–771.
14. Liu S, Yu M, Ye C, Lam DSC, Leung CK-S. Anterior chamber angle imaging with swept-source optical coherence tomography: an investigation on variability of angle measurement. *Invest Ophthalmol Vis Sci*. 2011;52:8598–8603.
15. Sakata LM, Lavanya R, Friedman DS, et al. Comparison of gonioscopy and anterior segment ocular coherence tomography in detecting angle closure in different quadrants of the anterior chamber angle. *Ophthalmology*. 2008;115:769–774.
16. Sharma R, Sharma A, Arora T, et al. Application of anterior segment optical coherence tomography in glaucoma. *Surv Ophthalmol*. 2014;59:311–327.
17. Maram J, Pan X, Sadda S, Francis B, Marion K, Chopra V. Reproducibility of angle metrics using the time-domain anterior segment optical coherence tomography: intra-observer and inter-observer variability. *Curr Eye Res*. 2015;40:496–500.
18. McKee H, Ye C, Yu M, Liu S, Lam DSC, Leung CKS. Anterior chamber angle imaging with swept-source optical coherence tomography: detecting the scleral spur, Schwalbe's Line, and Schlemm's Canal. *J Glaucoma*. 2013;22:468–472.
19. Pan X, Marion K, Maram J, et al. Reproducibility of anterior segment angle metrics measurements derived from cirrus spectral domain optical coherence tomography. *J Glaucoma*. September 2014.
20. Varma R, Hsu C, Wang D, Torres M, Azen SP. The Chinese American Eye Study: design and methods. *Ophthalmic Epidemiol*. 2013;20:335–347.
21. Ho S-W, Baskaran M, Zheng C, et al. Swept source optical coherence tomography measurement of the iris-trabecular contact (ITC) index: a new parameter for angle closure. *Graefes Arch Clin Exp Ophthalmol*. 2013;251:1205–1211.
22. Leung CK-S, Weinreb RN. Anterior chamber angle imaging with optical coherence tomography. *Eye (Lond)*. 2011;25:261–267.
23. Cicchetti DV. Guidelines, criteria, and rules of thumb for evaluating normed and standardized assessment instruments in psychology. *Psychol Assess*. 1994;6:284–290.
24. Blieden LS, Chuang AZ, Baker LA, et al. Optimal number of angle images for calculating anterior angle volume and iris volume measurements. *Invest Ophthalmol Vis Sci*. 2015;56:2842–2847.
25. Tun TA, Baskaran M, Perera SA, et al. Sectoral variations of iridocorneal angle width and iris volume in Chinese Singaporeans: a swept-source optical coherence tomography study. *Graefes Arch Clin Exp Ophthalmol*. 2014;252:1127–1132.
26. Tun TA, Baskaran M, Zheng C, et al. Assessment of trabecular meshwork width using swept source optical coherence tomography. *Graefes Arch Clin Exp Ophthalmol*. 2013;251:1587–1592.
27. He M, Foster PJ, Ge J, et al. Gonioscopy in adult Chinese: the Liwan Eye Study. *Invest Ophthalmol Vis Sci*. 2006;47:4772–4779.
28. Kunimatsu S, Tomidokoro A, Mishima K, et al. Prevalence of appositional angle closure determined by ultrasonic biomicroscopy in eyes with shallow anterior chambers. *Ophthalmology*. 2005;112:407–412.
29. Jing T, Marziliano P, Wong H-T. Automatic detection of Schwalbe's line in the anterior chamber angle of the eye using HD-OCT images. *Conf Proc IEEE Eng Med Biol Soc*. 2010:3013–3016.